ELSEVIER

Earth and Planetary Science Letters 154 (1998) 139–151

EPSL



# void–volatile self-lubrication

David Bercovici *

*Department of Geology and Geophysics, School of Ocean and Earth Science and Technology, University of Hawaii, 1680 East–West Road, Honolulu, HI 96822, USA*

Received 19 June 1997; revised 7 October 1997; accepted 7 October 1997

**Abstract**

The formation of plate tectonics from mantle convection necessarily requires nonlinear rheological behavior. Recent studies suggest that self-lubricating rheological mechanisms are most capable of generating plate-like motion out of fluid flows. The basic paradigm of self-lubrication is nominally derived from the feedback between viscous heating and temperature-dependent viscosity. Here, we propose a new idealized self-lubrication mechanism based on void (e.g., pore and/or microcrack) generation and volatile (e.g., water) ingestion. We test this void–volatile self-lubrication mechanism in a source–sink flow model; this leads to a basic nonlinear system which permits the excitation of strike–slip (toroidal) motion (a necessary ingredient of plate-like motion) out of purely divergent (i.e., poloidal or characteristically convective) flow. With relatively inviscid void-filling volatiles, the void–volatile mechanism yields a state of highly plate-like motion (i.e., with uniformly strong ''plate'' interiors, weak margins, and extremely focussed strike–slip shear zones). Moreover, the void–volatile model obeys a chemical diffusion time scale that is typically much longer than the thermal convection time scale; the model thus complies with the observation that plate boundaries are long lived and survive even while inactive. The void–volatile model of self-lubrication therefore predicts self-focussing shear zones, plate generation, and plate-boundary longevity through what has long been suspected to be a key ingredient for the existence of plate tectonics, i.e., water. © 1998 Elsevier Science B.V.

*Keywords:* plate tectonics; plates; mantle; convection; viscosity; strike-slip faults

## 1. Introduction

The manner in which plate tectonics is not only driven by, but generated from convection in the Earth's mantle is undoubtedly one of the most important issues remaining in the field of global geodynamics. A form of mantle convection with plate-like motion at the surface would necessarily have, among other features, an extensive amount of strike–slip or toroidal motion. The generation of toroidal motion has been the subject of numerous papers over the last two decades [1–10] as it is particularly anomalous for highly viscous buoyancy-driven flows. Toroidal motion requires nonlinear rheological behavior to indirectly draw energy from the mantle's release of gravitational potential energy; i.e., lateral viscosity variations cause the more purely convective poloidal (upwelling/downwelling and divergent) flow to generate vertical torques which drive toroidal motion. However, it has become abundantly clear in recent

* Corresponding author. E-mail: dberco@wai.soest.hawaii.edu


*PII* S0012-821X(97)00182-9

years that basic silicate non-Newtonian creep and/or diffusion rheologies are not sufficiently nonlinear in and of themselves to generate significant toroidal flow [8,11]. Highly non-Newtonian or other nonlinear rheological behavior is likely required to yield sufficiently plate-like strike–slip motion.

Various continuum mechanical models have tried to generate plate-like motion as an instantaneous response to convective flow through prescribed viscosity gradients [5] or non-Newtonian lithospheric rheology [7,8,12,13]. In these models, plate-like motion would exist as long as convective flow drives lithospheric deformation and causes weak zones; but once the convective currents responsible for this deformation stop or move away from the pseudo-plates, the plates cease to exist. However, Zhong and Gurnis [14] and Gurnis [15] recently pointed out the inadequacy of such instantaneous rheological responses because many plate boundaries arise by adopting intrinsically weak zones in the lithosphere left over from previous, even abandoned, boundaries (see also Hager and O'Connell [16]). That plate boundaries may be accumulated and recycled, that they survive even if there is no deformation across them, strongly suggests that they act on a time scale independent of the convective time scale. Thus the question of plate generation must be extended to concern not only how weak boundaries form, but how they persist through time even while inactive.

One nonlinear rheological mechanism which is time dependent in addition to permitting narrow self-focussing boundaries (strike–slip boundaries in particular) involves self-lubricating effects [10,17]. Such self-lubrication classically arises from the coupling of thermoviscous behavior and viscous heating [18]. However, the time-scale for this mechanism is the same as the convective scale (i.e., the thermal diffusion scale) and thus responds in parallel to changes in convection, not independently. (Other problems with the viability of the viscous-heating model are examined in this paper.) Moreover, thermally activated self-lubrication is likely not the only form of self-lubrication. Rheological mechanisms involving dynamic recrystallization and grain-size dependent viscosity may also provide the necessary shear-focussing effects [19–21]. However, with the presence of water on Earth, a self-lubrication mechanism based on ingestion of volatiles [22] — which have a chemical diffusion time scale orders of magnitude longer than the convective time scale [23] — is clearly worthy of examination.

In this paper we derive and examine a simplified self-lubrication model based on void generation and volatile ingestion (and henceforth refer to it as the *void–volatile* model). (This model differs significantly from volatile lubrication models which depend on the entrainment of hydrated sediments [22].) We compare this model to the analogous viscous-heating based model with a more realistic temperature-dependent viscosity law than used previously by Bercovici [10]. We infer that it is the void–volatile self-lubrication model which is most likely to yield plate-like motion with a distinct and potentially very long time scale, thus complying with evidence for the influence of water, and the longevity of plate boundaries.

## 2. Self-lubricating mechanisms

In this paper we consider two possible self-lubrication mechanisms. The first, involving the feedback between viscous heating and temperature-dependent viscosity, is the paradigm of self-lubrication; it has been applied to a variety of tectonic problems from asthenospheric flow [18], earthquake slider-block models [24] and most recently the excitation of toroidal motion in convection [17,25] and plate generation itself [10]. The other model, developed here, involves the feedback between formation of voids (pores and/or microcracks) via continuous deformation and subsequent volatile ingestion. The latter is an idealized model somewhat related to the concepts of ductile void growth [26–28]; here, we construct a deterministic set of equations for void formation and volatile ingestion analogous to (and to a large extent guided by) the equations for the viscous-heating based mechanism. The importance of either self-lubrication mechanism for the plate generation problem is that they provide the viscosity variability through which toroidal or strike–slip motion can draw energy from the poloidal field. Below we briefly outline the viscous-heating self-lubrication mechanism, and then present a detailed derivation of the void–volatile mechanism.

### 2.1. Viscous heating and thermoviscous behavior

The theoretical model describing self-lubrication due to viscous heating and temperature-dependent viscosity has been described elsewhere numerous times and in sufficient detail [10,17,18] to warrant only a brief summary of the basic equations. Our theory follows the development proposed by Bercovici [10]. All variables and equations presented in this section are already dimensionless; the dimensional scales are stated in Bercovici [10].

In Bercovici [10], we considered only a linearly temperature-dependent viscosity to provide the minimum level of complexity. To test the effect of this simplifying assumption, we will, in this paper, use a more realistic exponential law

$$\mu(\Theta) = \mathrm{e}^{-\nu\Theta} \tag{1}$$

where $\mu$ is the dimensionless viscosity, $\Theta$ the dimensionless temperature anomaly, and $\nu$ the dimensionless viscosity variability (see Table 1).

In our model we consider only horizontal two-dimensional flow in a thin layer. Herein the temperature anomaly is generated by viscous heating, and diffused and transported according to the vertically averaged conservation law

$$\frac{\partial\Theta}{\partial t} + \mathrm{v_h}\cdot\nabla_\mathrm{h}\Theta = -\Theta + \nabla_\mathrm{h}^2\Theta + \mu(\Theta)\dot{e}^2 \tag{2}$$

where $\mathrm{v_h}$ is the horizontal velocity vector, $\nabla_\mathrm{h}$ is the horizontal gradient operator, and $\dot{e}^2$ is the second strain-rate invariant [7,10]. The last term on the right-hand side of Eq. (2) is viscous heating, while the other terms represent the standard forms of temporal change, advection and diffusion (the first term on the right represents vertical diffusion).

A scaling analysis of Eq. (2) with Eq. (1) leads to an equation for the scale of the maximum temperature anomaly $\Theta_\mathrm{max}$:

$$\Theta_\mathrm{max}\,\mathrm{e}^{\nu\Theta_\mathrm{max}} = \tau\dot{e}_\mathrm{max}^2 \tag{3}$$

where $\tau$ is the harmonic average of the secular, advective and diffusion time scales. We solve Eq. (3) numerically for $\Theta_\mathrm{max}$ and use the solution to obtain a constitutive relation, i.e., a stress scale $\sigma_\mathrm{max} = \mu(\Theta_\mathrm{max})\dot{e}_\mathrm{max}$ as a function of a strain-rate scale $\dot{e}_\mathrm{max}$ (Fig. 1). Clearly, the viscous-heating based mechanism with the exponential viscosity law displays the classic features of self-lubrication or stick–slip behavior; i.e., stress reaches a peak value at a given strain-rate after which, at higher strain-rates, the stress decreases [7–10,24]. Thus at high enough strain-rates the medium not only becomes less viscous as it is deformed more rapidly, it also offers less resistance to deformation and essentially lubricates itself.

### 2.2. Void generation and volatile ingestion

While the coupling of viscous heating and thermoviscous behavior is the basic paradigm of self-lubrication, it is certainly not the only form of self-lubrication. Here, we consider a self-lubrication mechanism based on the production of voids (i.e., microcracks and pores) and subsequent volatile ingestion in continuously deforming materials. Void growth in ductile media has been studied in the metallurgical and ceramic sciences [26,27] especially in regard to its influence on plastic failure. A recent study [28] applied the theory of dilatant plasticity and ductile void growth to a region of intraplate deformation in the European plate with quite promising results.

In this paper we deduce an idealized theory for void growth in a viscous medium. We present a very simple model for the viscosity of a medium with saturated voids, and a transport law for the void density (i.e., porosity). However, it should be well understood that the point of this model is to write down the simplest possible equations which describe the essence of such void–volatile self-lubrication. Several simplifying assumptions are made and these are discussed in some detail in order to suggest potential improvements, expansions and future avenues of research.

#### 2.2.1. Viscosity law

Determination of the effective viscosity of continua with two or more phases or components is, in

Table 1
Dimensionless variables and constants for the governing equations

| Variables | | | |
|---|---|---|---|
| Symbol | Definition | Ref. eqns. | Model |
| $\Theta$ | temperature anomaly | Eq. (2) | viscous heating |
| $\Phi$ | void density (porosity) | Eq. (8) | void–volatile |
| $\mu$ | viscosity | Eq. (1), Eq. (9) | both |
| $\phi$ | poloidal velocity potential | Eq. (14), Eq. (15) | both |
| $\psi$ | toroidal stream function | Eq. (14), Eq. (16) | both |
| $S$ | shape of source–sink field | Eq. (15) | both |

| Constants | | | |
|---|---|---|---|
| Symbol | Definition | Value | Model |
| $\nu$ | exponential viscosity variability | 0–5000 | viscous heating |
| $\lambda$ | linear viscosity variability | 0–1 | void–volatile |
| $\eta$ | susceptibility to void generation | 0–4600 | void–volatile |
| Pe | source-sink Péclet number (flow rate) | 1 | both |
| $\delta$ | source or sink half-width | 2 | both |
| $\alpha$ | half-length of and half-spacing between source and sink | 50 | both |

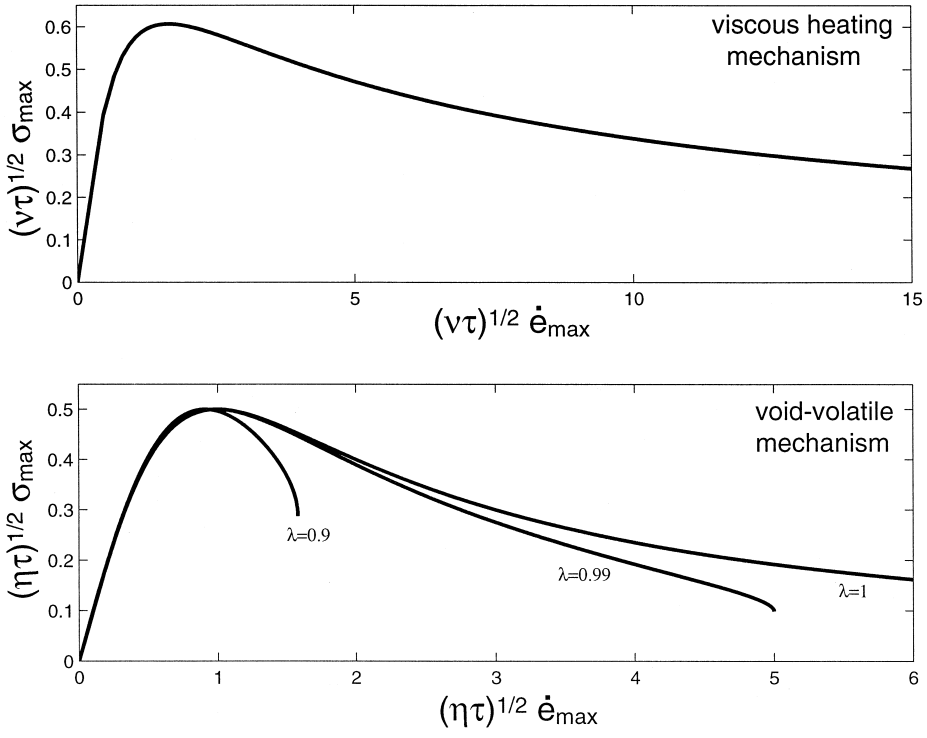


Fig. 1. Dimensionless stress scale vs. strain-rate scale for the viscous-heating based self-lubrication mechanism with exponentially temperature-dependent viscosity (*top frame*); and the void–volatile mechanism for three different values of $\lambda$, indicated on the figure (*bottom frame*). For the viscous-heating based model, stress and strain-rate are re-scaled by the factor $(\nu\tau)^{1/2}$, in which case all solutions (regardless of $\nu$ and $\tau$) collapse to one curve; this follows from the fact that, on inspection of Eq. (3), the re-scaled variable $\nu\theta_{max}$ is a function of only $\nu\tau\dot{e}^2_{max}$. For the void–volatile model, stress and strain-rate are re-scaled by $(\eta\tau)^{1/2}$ to yield curves that are independent of $\eta$ and $\tau$ (this follows from Eq. (10)] which shows that $\Phi_{max}$ is a function of only $\epsilon^2 = \eta\tau\dot{e}^2_{max}$ and $\lambda$). See text for further discussion.

general, a highly complex problem. Lacking any comprehensive viscosity law, we adopt here the simplest possible approach to estimate the essential rheological behavior.

The minimum constraints we can place on a law for effective viscosity as a function of porosity $\Phi$ is that the viscosity equals exactly the porous matrix viscosity $\mu_m$ when $\Phi = 0$, and exactly the volatile viscosity $\mu_v$ when $\Phi = 1$. A simple estimate of the effective viscosity can be obtained by considering the viscous dissipation in the two-component medium driven by a steady-state strain-rate field [29]. Neglecting strain-rate perturbations (which are analytically intractable unless the two-component system is a dilute suspension), the ratio of viscous dissipation (averaged over a small control volume) to the second strain-rate invariant (averaged over the same volume) leads to an effective viscosity

$$\mu = \mu_m(1 - \lambda\Phi) \tag{4}$$

where $\lambda = (\mu_m - \mu_v)/\mu_m$ (note we are, for the moment, using dimensional viscosity). Eq. (4) is clearly the simplest viscosity law satisfying the minimum constraints. While a more rigorous determination of a viscosity law requires an empirical determination, preliminary numerical studies of deformable porous media suggest that a linear law is in fact a reasonably good approximation [30]. In this study we assume that voids are not interconnected (see below), at least until $\Phi = 1$, as might be expected in a foam; thus, unlike a partial melt, there is no critical porosity at which disaggregation of the matrix and precipitous drops in viscosity occur.

*2.2.2. Void evolution*

In this section we derive a conservation law for voids that are generated by the continuous deformation of our ''lithospheric'' medium. We assume that the voids are all instantaneously and continuously saturated with volatile for which there is essentially an inexhaustible supply (e.g., the ocean).

As noted above, we consider two-dimensional horizontal flow in a thin-layer. Our transport law is averaged over the layer thickness and has the general form of

$$\frac{\partial\Phi}{\partial t} + \mathbf{v}_h \cdot \nabla_h\Phi = Q_+ - Q_- \tag{5}$$

where $Q_+$ and $Q_-$ represent sources and sinks of voids, respectively, and $\Phi$ is now the vertically averaged porosity. (Again, for the moment, we are using dimensional variables, until we determine the proper length and time scales with which to nondimensionalize our void generation model). In writing the left-hand side of Eq. (5) we assume: (1) that voids are not interconnected (thus matrix permeability is zero), and therefore there is no relative motion between the volatiles and porous matrix; and (2) that our medium remains effectively incompressible, even while it is forming voids. We assume that compressibility effects are secondary to the self-lubrication mechanism and avoid the issue by assigning the void-filling fluid a density equal to the matrix density (although the fluid and matrix may have very different viscosities) [31]. The elimination of compressibility excludes extra sources of velocity divergence which are presently of no concern to us since, in our source–sink model (see below), we completely prescribe the divergence field. This assumption keeps our model analysis as basic as possible; however, we note that such compressibility effects are worthy of exploration in future studies with more sophisticated models.

We next deduce appropriate sources and sinks for the void generation equation. Loss of voids is likely to occur through: (1) molecular diffusion of void liquids into the surrounding matrix (e.g., through hydration), with subsequent loss of pore pressure to maintain the voids; and (2) diffusion or dissolution and subsequent precipitation of matrix minerals into the void liquid, leading to healing or annealing of the voids. In either case we assume the void sink appears as a standard diffusion term with a chemical diffusivity $\beta$. Averaged over the layer depth, this diffusive sink term becomes

$$Q_- = -\frac{C\beta}{H^2}\Phi + \beta\nabla_h^2\Phi \tag{6}$$

where $H$ is the layer thickness, and $C$ is a dimensionless constant depending on the geometry of the vertical porosity profile (e.g., if porosity goes parabolically from 1 at the surface, $z = 0$, to 0 at the base of the layer, $z = -H$, then $C = 3$).

For the source term $Q_+$ we assume that the rate at which voids are created depends on the deviatoric

stress tensor $\sigma_{ij}$ (i.e., should depend on the stress in excess of a confining isotropic stress or pressure). As with brittle and ductile void or microcrack nucleation [28,32] we assume that voids are generated for all nonzero deviatoric stresses, not just for those stresses exceeding some critical yield or failure criterion. Since the transport law for void density is a scalar equation, our source term is necessarily an invariant, and thus we assume is proportional to the second deviatoric stress invariant $\sigma_{ij}\sigma_{ij} = 4\mu_m^2(1-\lambda\Phi)^2\dot{e}^2$. (This differs somewhat from ductile void growth theory for reasons discussed below.) However, the validity of our isotropy assumption is certainly worthy of future study.

Finally, the source term controlling void generation must incorporate the weakening effect due to thinning of matrix walls (separating the voids) as the void population grows; i.e., for a given stress state the susceptibility to forming voids necessarily increases as the matrix becomes more fragile. Therefore the source term must also contain a fragility factor proportional to $(1-\Phi)^{-1}$ (see also [28]). In total, we employ a source or damage term that takes the form

$$Q_+ = \Gamma\frac{\mu_m^2(1-\lambda\Phi)^2\dot{e}^2}{(1-\Phi)} \tag{7}$$

where $\Gamma$ is a constant. The fragility factor $(1-\Phi)^{-1}$ serves an additional vital role: while it becomes singular at $\Phi = 1$ (i.e., infinitely fragile) it also eliminates the unphysical formation of $\Phi > 1$. That is, if $\Phi$ exceeds unity for numerical reasons, the source term becomes a sink and unphysical values of $\Phi$ are forced to vanish.

Our model is considerably simpler than ductile void growth theory [28] which generally accounts for void–void interactions beyond a critical porosity [33] and has separate but coupled equations for void nucleation and growth. (Growth of void size is essentially neglected in our model, though the density of voids can hypothetically grow to permit $\Phi = 1$.) Moreover, void nucleation rate in fully ductile flow is postulated to depend on strain-energy rate $\sigma_{ij}\dot{e}_{ij} = 2\mu\dot{e}^2$, instead of the stress invariant $\sigma_{ij}\sigma_{ij}$ which is more generally used for brittle void generation; more sophisticated (and hence more parameter dependent) models employ both effects with some transition at a critical state [28,34]. However, if we were to replace the stress invariant in Eq. (7) with the strain-energy rate, then, in the limit of inviscid void fluid ($\lambda = 1$), we would obtain the unphysical result that void generation would depend only on $\dot{e}^2$; since the source term would be positive definite for all values of $\Phi$, then voids could be generated without bounds on $\Phi$ (i.e., a $\Phi > 1$ would be allowed), and the self regulation due to diminishing viscosity would be nullified. Of course, this physical inconsistency might also be mitigated by permitting nonlinearities in the viscosity law or fragility factor. These issues all emphasize the problematic nature of modelling void generation and damage (see also Sleep [35]); invariably, much more of the physics of these processes needs to be elucidated through experimental studies.

Following the nondimensionalization scheme for the viscous-heating based self-lubrication model [10], we nondimensionalize length by $H/\sqrt{C}$, time by $H^2/C\beta$ and viscosity by $\mu_m$. This leads to a dimensionless version of our transport law [i.e., Eq. (5) with Eqs. (6) and (7)]

$$\frac{\partial\Phi}{\partial t} + \mathrm{v}_h\cdot\nabla_h\Phi = -\Phi + \nabla_h^2\Phi + \eta\frac{(1-\lambda\Phi)^2\dot{e}^2}{(1-\Phi)} \tag{8}$$

where $\eta = \Gamma\mu_m^2 C\beta/H^2$. The definitions of $\Phi$ and $\lambda$ do not change since they were originally dimensionless. However, our dimensionless viscosity is

$$\mu(\Phi) = 1-\lambda\Phi\,. \tag{9}$$

(See Table 1 for a list of variables and constants.)

In the limit that the ingested volatile is relatively inviscid, i.e., $\lambda = 1$, Eq. (8) is mathematically identical (with the substitutions $\Phi = \nu\theta$ and $\eta = \nu$) to the temperature equation from the simplified viscous-heating model of Bercovici [10] which used a linearly temperature-dependent viscosity.

### 2.2.3. Scale analysis of void generation model

A scale analysis of Eq. (8) leads to an equation for the scale of the maximum porosity anomaly $\Phi_{max}$:

$$\frac{\Phi_{max}}{\tau} = \eta\frac{(1-\lambda\Phi_{max})^2\dot{e}_{max}^2}{(1-\Phi_{max})} \tag{10}$$

where $\tau$ is again the harmonic average of the secular, advective and diffusion time scales. For $\lambda = 1$ this leads to

$$\Phi_{\max} = \frac{\epsilon^2}{1+\epsilon^2} \tag{11}$$

where $\epsilon^2 = \tau\eta\dot{e}^2_{\max}$. For $\lambda < 1$ we find

$$\Phi_{\max} = \frac{1 + 2\lambda\epsilon^2 - \sqrt{1 - 4(1-\lambda)\epsilon^2}}{2(1+\lambda^2\epsilon^2)} \tag{12}$$

where we choose only one of the roots to Eq. (10) such that voids are only created if the medium is being deformed (i.e., $\Phi_{\max} = 0$ when $\epsilon^2 = 0$).

For $\lambda = 1$ any value of $\epsilon^2$ between 0 and $\infty$ is allowed; for these $\epsilon^2$ the corresponding $\Phi_{\max}$ would be between 0 and 1. However, for $\lambda < 1$ not all values of $\epsilon^2$ are allowed; i.e., real values of $\Phi_{\max}$ exist only for

$$\epsilon^2 \le [4(1-\lambda)]^{-1} \tag{13}$$

in which case the maximum allowable value of $\Phi_{\max}$ is $(2-\lambda)^{-1}$. For larger values of $\epsilon^2$ the source term [right-hand side of Eq. (10)] cannot be balanced by the sink terms, causing $\Phi_{\max}$ to undergo run-away growth to its maximum value of 1. However, while $\Phi_{\max} = 1$ is a fixed point (i.e., the source term is positive for $\Phi < 1$ but negative for $\Phi > 1$) it is, for $\lambda < 1$, a singular fixed point (i.e., the source term is singular) at which no physical solution exists. Thus, the scaling analysis suggests that for $\lambda < 1$ stable solutions only exist with $\Phi < 1$ for limited values of $\epsilon^2$; however, for $\lambda = 1$ the singular nature of the source term vanishes and solutions with $\Phi = 1$ are allowed and solutions exist for any value of $\epsilon^2$. We find this feature to be quite relevant to our numerical experiments.

Fig. 1 shows, for different values of $\lambda$, the stress scale $\sigma_{\max} = (1 - \lambda\Phi_{\max})\dot{e}_{\max}$ vs. strain-rate scale $\dot{e}_{\max}$. (The curves for $\lambda < 1$ are truncated since, as noted above, they do not exist for $\epsilon > [4(1-\lambda)]^{-1/2}$.) For values of $\lambda$ less than $\sim 0.3$, the stress–strain-rate constitutive relation is largely linear for the allowed strain-rates. For larger values of $\lambda$ a maximum stress is achieved at a cut-off strain-rate, beyond which stress decreases with strain-rate as with other self-lubrication mechanisms.

## 3. Flow model

To test the ability of the various self-lubrication mechanisms to generate plate-like motion, we employ the same simple source–sink flow model we have used previously [7–10]. One of the main issues of plate generation, as has been discussed extensively before, is how toroidal (strike–slip) motion is generated from the coupling of poloidal (divergent) flow with rheological nonlinearities. The assumed source–source sink field (Fig. 2, top) represents a simple model of poloidal motion (whose causes are already reasonably well elucidated by basic convection studies); when this is coupled to our self-lubrication rheological mechanism, toroidal motion is generated. Whether the toroidal motion generated is plate-like (i.e., concentrated into narrow zones of shear or vertical vorticity) depends largely on the parameters of the self-lubrication model.

In this paper we use simple shallow-layer, Cartesian, viscous and incompressible flow to model motion for either self-lubrication mechanism. In using this flow model for the void–volatile mechanism, we assume, as stated above, that the voids are not interconnected (and thus there is no relative motion between volatile fluid and matrix), and that the volatile and matrix have equal density. (A more sophisticated model could possibly separate the motion of the matrix and volatile using Darcy flow, and employ compressible viscous fluid dynamics for matrix deformation, similar to the formulations for magma transport [31].) The equations for the flow model used here have been fully developed elsewhere [7,10]. We briefly discuss the essential nondimensional equations for completeness. Horizontal 2-D velocity is given by a Helmholtz representation

$$\mathbf{v}_h = \nabla_h\phi + \nabla_h \times (\psi\hat{z}) \tag{14}$$

where $\phi$ is the poloidal scalar potential, $\psi$ is the toroidal stream function, and $\hat{z}$ is the unit vector in the vertical direction. The source–sink field is a prescribed horizontal divergence which yields an equation for $\phi$:

$$\nabla_h \cdot \mathbf{v}_h = \nabla_h^2\phi = \frac{\mathrm{Pe}}{\delta} S(x,y) \tag{15}$$

where Pe is the Péclet number, which determines the velocity of the source–sink flow, $\delta$ is the half-width of either the source or sink, and $S(x,y)$ is a function

which defines the shape of the source–sink field. The source and sink are each narrow elongated regions of positive and negative divergence, respectively; they are mathematically defined as hyperbolic-secants (of half-width $\delta$), truncated in length to be $2\alpha$ long (by using hyperbolic-tangents); the centers of the source and sink are also separated perpendicular to their long axes by $2\alpha$. [This source–sink field in fact derives from the divergence of the motion of a simple square plate of sides $2\alpha$ [7,10].] We defer to Bercovici [7,10] for more detailed discussion of the source–sink field; however, the top frame of Fig. 2 should make the appearance of the source–sink field fairly obvious.

The toroidal stream function $\psi$ is found through the equation of motion for shallow-layer creeping flow with variable viscosity; as shown by Bercovici [7] this leads to

$$\mu\nabla_h^4\psi + 2\nabla_h\mu\cdot\nabla_h\nabla_h^2\psi + \Delta^*\mu\Delta^*\psi + 4\frac{\partial^2\mu}{\partial x\partial y}\frac{\partial^2\psi}{\partial x\partial y} = \hat{z}\cdot\nabla_h\mu\times\nabla_h\nabla_h^2\phi + 2\Delta^*\mu\frac{\partial^2\phi}{\partial x\partial y} - 2\frac{\partial^2\mu}{\partial x\partial y}\Delta^*\phi \quad (16)$$

where $\mu$ is the variable viscosity (i.e., temperature- or porosity-dependent) discussed in previous sections, and $\Delta^* = \partial^2/\partial x^2 - \partial^2/\partial y^2$. Finally, given the velocity field described by Eq. (14), the second strain-rate invariant used in the self-lubrication models is

$$\dot{e}^2 = 2\left[\left(\frac{\partial^2\phi}{\partial x^2} + \frac{\partial^2\psi}{\partial x\partial y}\right)^2 + \left(\nabla_h^2\phi\right)^2 - \nabla_h^2\phi\left(\frac{\partial^2\phi}{\partial x^2} + \frac{\partial^2\psi}{\partial x\partial y}\right)\right] + \frac{1}{2}\left(2\frac{\partial^2\phi}{\partial x\partial y} - \Delta^*\psi\right)^2 \quad (17)$$

In the end, the governing equations are Eqs. (15) and (16) and either Eqs. (1) and (2) for thermal self-lubrication, or Eqs. (8) and (9) for void–volatile self-lubrication (see Table 1).

## 4. Numerical experiments

We examine a variety of numerical solutions to explore: (1) the effect of a more realistic temperature-dependent viscosity law than used in Bercovici [10]; and (2) the nature of the void–volatile self-lubrication mechanism.

The numerical solutions are obtained using a spectral-transform method described previously [7,10]. Our primary goal is to test the self-lubrication mechanisms, thus we leave the flow kinematics unchanged for all cases. That is, we use $\mathrm{Pe} = 1$, $\delta = 2$ as in Bercovici [10], and $\alpha = 50$ (which is larger than used previously, but is perhaps more representative of large plates like the Pacific than were the cases used by Bercovici [10]). The calculation domain is for $-100 \le x, y \le 100$. The majority of calculations were done on a $256 \times 256$ spatial grid; however, particularly plate-like and fine-scale solutions were verified on a $512 \times 512$ grid (and similar solutions were verified by Bercovici [10] on a $1024 \times 1024$ grid). We must caution that while the thermal self-lubrication mechanism has a time scale related to thermal diffusion [10], the void–volatile mechanism has a time scale that is very different, as it is based essentially on chemical diffusion. However, for the sake of comparison we use the same value of Pe for both self-lubrication mechanisms, and note that a more direct application to the Earth may require different parameter values.

### 4.1. Thermal self-lubrication results

A sample result for our viscous-heating based model is presented in Fig. 2 (case A) which shows velocity $\mathrm{v}_h$, vertical vorticity

$$\omega_z = \hat{z}\cdot\nabla_h\times\mathrm{v}_h = -\nabla_h^2\psi \quad (18)$$

(which measures the rate of strike–slip shear and is positive for left-lateral or counter-clockwise shear

Fig. 2. The source–sink field (*top frame*); also the velocity (*left-hand column*), vorticity (*middle column*) and temperature or porosity (*right-hand column*; the relevant variable is indicated beside the *color scale*) for selected cases (indicated at the far left). Case A is for the viscous-heating based self-lubrication mechanism with exponentially temperature-dependent viscosity and $\nu = 2000$. Case B is for the void–volatile self-lubrication mechanism with $\lambda = 0.999$ and its maximum allowable value of $\eta = 1840$. Case C is for the void–volatile mechanism with $\lambda = 1$ and $\eta = 2000$.

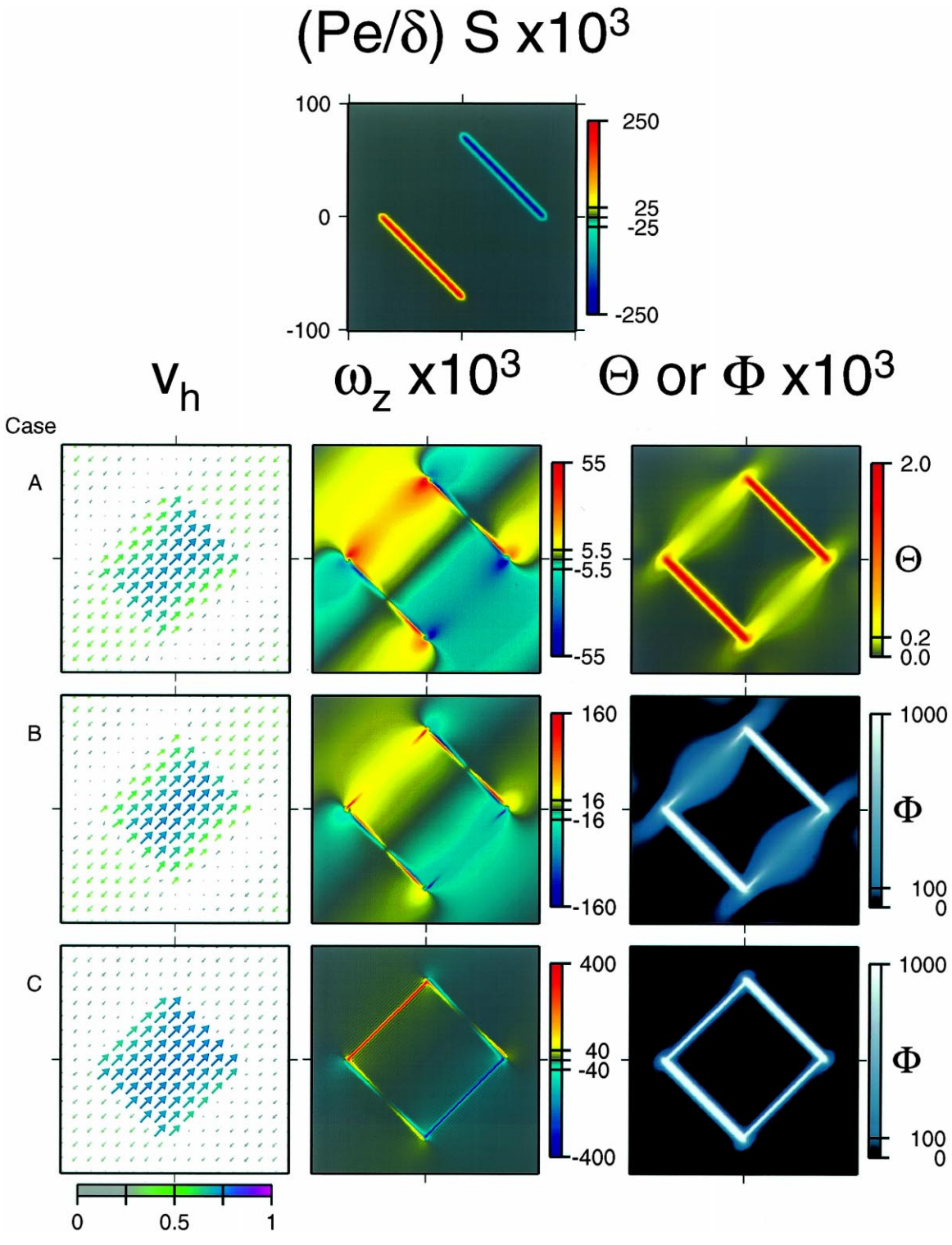
(Pe/δ) S x10³
100
0
-100
250
25
-25
-250
v_h
ω_z x10³
Θ or Φ x10³
Case
A
B
C
55
5.5
-5.5
-55
2.0
Θ
0.2
0.0
160
16
-16
-160
1000
Φ
100
0
400
40
-40
-400
1000
Φ
100
0
0
0.5
1

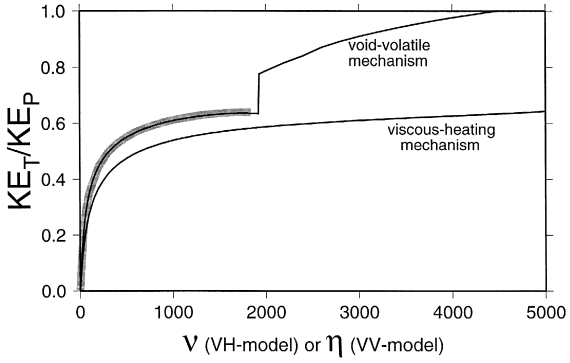


Fig. 3. Toroidal–poloidal energy ratio $KE_T/KE_P$ vs. $\nu$ for the viscous heating based (VH) self-lubrication model, or $\eta$ for the void–volatile (VV) model (as indicated). The void–volatile curves show values for both $\lambda = 0.999$ (*thick gray curve*) and $\lambda = 1$ (*overlying, narrow black curve*).

and negative for right-lateral shear) and temperature anomaly $\Theta$ for $\nu = 2000$. It is evident that even for high values of $\nu$, the strike–slip shear zones are relatively un-plate-like and diffuse. These solutions were calculated from $\nu = 1$ to $\nu = 5000$ with relatively little change for $\nu > 1000$; for all cases there was no particularly plate-like state.

The toroidal–poloidal kinetic energy ratio

$$\frac{KE_T}{KE_P} = \frac{\int_A \nabla_h \psi \cdot \nabla_h \psi \, dx dy}{\int_A \nabla_h \phi \cdot \nabla_h \phi \, dx dy} \qquad (19)$$

(where $A$ is the area of the 2-D domain) measures the relative amount of bulk toroidal motion. For an ideal square plate this ratio would be unity [7,10]; thus attaining a unity ratio with our continuum mechanical model is desirable. $KE_T/KE_P$ increases with $\nu$ rapidly (Fig. 3) for $\nu \leq 500$. For larger $\nu$, $KE_T/KE_P$ increases only gradually with increasing $\nu$, suggesting that it cannot reach a plate-like value of unity.

### 4.2. Void-volatile self-lubrication results

Several series of steady-state solutions were calculated for different values of $\lambda$ and $\eta$ for the void–volatile model. For all cases with $\lambda < 1$ steady solutions exist only for values of $\eta$ less than some critical value. Above this critical $\eta$ (which increases with increasing $\lambda$), solutions (even time-dependent ones) could not be found. In fact, the lack of solutions above the critical $\eta$ is in keeping with our previous scaling analysis.

Fig. 2 (case B) shows a sample steady solution at $\lambda < 1$; in particular we use $\lambda = 0.999$ at the maximum allowable value of $\eta = 1840$ in order to obtain a large viscosity contrast. It is clear that, for the allowable steady solutions, the toroidal motion is diffuse and un-plate-like, although it has more plate-like concentrations of vorticity than the viscous-heating based model.

We finally consider cases for which the void-filling volatile is inviscid, i.e., $\lambda = 1$. As solutions to this case are found with increasing $\eta$, the toroidal motion differs little from the case with $\eta = 0.999$. However, at $\eta = 1920$, a bifurcation occurs in the solutions to a highly plate-like state; the plate-like state persists and becomes even more plate-like as $\eta$ increases past 1920. Fig. 2 (case C) shows that the solution for $\nu = 2000$ has a very plate-like velocity field; this is emphasized by the vorticity field which is concentrated into extremely narrow continuous zones connecting the ends of the source and sink. The regions of high vorticity appear by all definitions to have the character of strike–slip faults. Moreover, the porosity field is also concentrated in narrow and straight anomalies; as these represent low-viscosity zones they show a contiguous and narrow weak margin surrounding a strong and square plate. For all values of $\eta$ above the bifurcation point, the maximum porosity remains at $\Phi = 1$. The porosity maxima themselves are associated with the fault-like strike–slip shear zones, and, given that $\lambda = 1$, these shear zones thus have zero viscosity. The regions of concentrated vorticity are essentially faults with zero strength.

Fig. 3 shows the kinetic energy ratio $KE_T/KE_P$ vs. $\eta$ for the two cases with $\lambda = 0.999$ and $\lambda = 1$. For the case with $\lambda < 1$, $KE_T/KE_P$ increases rapidly for $\eta < 500$, but appears to saturate for higher $\eta$ until the solutions reach the maximum allowable value of $\eta = 1840$. For the case with $\lambda = 1$, $KE_T/KE_P$ behaves similarly to the case with $\lambda = 0.999$, but undergoes a very large jump to $\sim 0.8$ at the bifurcation point of $\eta = 1920$. For $\eta > 1920$, $KE_T/KE_P$ climbs rapidly with increasing $\eta$ and actually reaches unity at $\eta = 4600$.

As noted previously, the solutions to the void–volatile model for $\lambda = 1$ are mathematically identical

within a constant to solutions one would obtain using the Bercovici [10] viscous-heating model with a linearly temperature-dependent viscosity. Thus, although the physics, calculations and geometries are different, the bifurcation shown here is mathematically closely related to the bifurcation reported by Bercovici [10].

## 5. Discussion

The analyses presented here indicates that, for the viscous-heating based self-lubrication mechanism with a realistic exponentially temperature-dependent viscosity, the plate-like state appears not to exist. A plate-like state does occur in the void–volatile model, but only if the void-filling fluid is effectively inviscid ($\lambda = 1$); such a situation, however, is physically plausible since the most likely volatile, i.e., water, has a viscosity that is at least $10^{25}$ times less viscous than lithospheric material. It is important to note that the bifurcation to plate-like motion in the case with $\lambda = 1$ is marked by shear zones reaching a porosity of $\Phi = 1$, and therefore having zero viscosity and no strength. It is at this limit of an inviscid shear zone that the shear-rate (and hence vorticity) must essentially become singular to satisfy the equations of motion. That the model reproduces nearly singular faults with zero strength is in basic agreement with Zhong and Gurnis [14] who found their most plate-like lithospheric flow when their imposed faults had zero strength or friction.

As noted by Bercovici [10] the solutions in the highly plate-like state have shear zones that are suggestive of plate-like singularities. However, singularities are, strictly speaking, not completely resolvable with numerical methods (unless treated as a priori boundary conditions), especially spectral methods. Clearly we have reached the limit at which continuum mechanics fails and thus our continuum model can only strongly suggest the formation of singular plate boundaries, but it cannot in fact resolve them exactly. However, while the standard model of plate tectonics does employ discontinuous plates with singular, zero-strength boundaries, the Earth's lithosphere is not in fact discontinuous; many plate margins have finite width and strength, as evident by intraplate deformation and seismicity [36]. Thus singular plate boundaries may be an unattainably extreme, if not unrealistic, goal for plate generation models.

## 6. Conclusions

The simple theory presented here suggests that a possible necessary condition for the generation of plate tectonics from mantle flow is self-lubrication due to void generation and volatile ingestion. While self-lubrication due thermoviscous behavior and viscous heating is the original paradigm of self-lubrication, it does not appear by itself — with realistic rheologies — to offer a plausible mechanism for self-focussing shear zones. (However, recent work on the interaction between grain-size dependent viscosity [19] and viscous heating shows fairly promising shear localization effects [21].)

The role of volatiles implied by this study is in agreement with hypotheses about the probable role of water on Earth. As has been suggested several times in the last decade [22,37], a necessary condition for plate tectonics is very likely the presence of water, given: (1) the lubricating effects of water and hydrated sediments; (2) its reduction of melting temperatures at ridges; (3) the preponderance of submarine plate boundaries and the presence of very few active continental plate boundaries; and (4) the lack of Earth-like plate tectonics on the other terrestrial planets all of which are presently likely devoid of liquid water at the surface [38]. While natural models of plate tectonics found in lava lakes [39] and wax models [40] are also devoid of liquid water, they involve large supplies of a very low-viscosity molten phase which could quite easily play the role of low-viscosity liquid in the void–volatile mechanism.

The void–volatile self-lubrication model also complies with the recent suggestion by Zhong and Gurnis [14] and Gurnis [15] that plate boundaries adopt old intrinsic weaknesses left from previous plate boundaries; thus plate formation is ''history'' dependent in that the weak boundaries obey a different time scale from thermal convection. The void–volatile model provides a mechanism by which the original boundaries cannot only form but continue to survive; i.e., the boundaries' time scale would be governed by chemical diffusion of volatiles which is typically a much longer process than even thermal diffusion. (For example, diffusivity of water through

silicates ranges between $10^{-18}$ and $10^{-11}$ $m^2/s$, depending on the silicate mineral [23], as opposed to a typical silicate thermal diffusivity of $10^{-6}$ $m^2/s$.) Finally, with the void–volatile self-lubrication mechanism, once deformation on an abandoned boundary starts anew, its intrinsic weakness (due to voids and volatiles) is reset and refocussed, and any diffusion of the boundary since it was abandoned is effectively erased.

Although the void–volatile self-lubrication model presented here is clearly idealized, it potentially offers a viable avenue for future studies of the origin of plates and plate boundaries. This model shows reasonable promise because it allows highly plate-like states, and is in accord with basic inferences about the apparent necessary conditions for plate tectonics (i.e., the presence of water and occurrence of long-lived boundaries). In the end, the proposed model may offer a plausible and tractable method by which mantle convection models can self-consistently generate plate tectonics.

## Acknowledgements

The author thanks Klaus Regenauer-Lieb, Mike Gurnis, Shijie Zhong, Neil Ribe, Paul Tackley, Marc Spiegelman, Steve Martel and David Yuen for extremely helpful discussions, suggestions and/or reviews. This work was supported by NSF grant EAR-9458405. *[RV]*

## References

[1] W.M. Kaula, Material properties for mantle convection consistent with observed surface fields, J. Geopys. Res. 85 (1980) 7031–7044.
[2] A.M. Forte, W.R. Peltier, Plate tectonics and aspherical earth structure: The importance of poloidal–toroidal coupling, J. Geophys. Res. 92 (1987) 3645–3679.
[3] C.W. Gable, R.J. O'Connell, B.J. Travis, Convection in three dimensions with surface plates: Generation of toroidal flow, J. Geophys. Res. 96 (1991) 8391–8405.
[4] R.J. O'Connell, C.W. Gable, B.H. Hager, Toroidal–poloidal partitioning of lithospheric plate motion, in: R. Sabadini, et al. (Eds.), Glacial Isostasy, Sea Level and Mantle Rheology, Kluwer, Norwell, MA, 1991, pp. 535–551.
[5] N.M. Ribe, The dynamics of thin shells with variable viscosity and the origin of toroidal flow in the mantle, Geophys. J. Int. 110 (1992) 537–552.
[6] C. Lithgow-Bertelloni, M.A. Richards, Y. Ricard, R.J. O'Connell, D.C. Engebretson, Toroidal–poloidal partitioning of plate motion since 120 Ma, Geophys. Res. Lett. 20 (1993) 375–378.
[7] D. Bercovici, A simple model of plate generation from mantle flow, Geophys. J. Int. 114 (1993) 635–650.
[8] D. Bercovici, A source–sink model of the generation of plate tectonics from non-Newtonian mantle flow, J. Geophys. Res. 100 (1995) 2013–2030.
[9] D. Bercovici, On the purpose of toroidal flow in a convecting mantle, Geophys. Res. Lett. 22 (1995) 3107–3110.
[10] D. Bercovici, Plate generation in a simple model of lithosphere–mantle flow with dynamic self-lubrication, Earth Planet. Sci. Lett. 144 (1996) 41–51.
[11] U. Christensen, H. Harder, Three-dimensional convection with variable viscosity, Geophys. J. Int. 104 (1991) 213–226.
[12] S. Weinstein, P. Olson, Thermal convection with non-Newtonian plates, Geophys. J. Int. 111 (1992) 515–530.
[13] S. Weinstein, Thermal convection in a cylindrical annulus with a non-Newtonian outer surface, Pure Appl. Geophys. 146 (1996) 551–572.
[14] S. Zhong, M. Gurnis, Interaction of weak faults and non-Newtonian rheology produces plate tectonics in a 3D model of mantle flow, Nature (London) 383 (1996) 245–247.
[15] M. Gurnis, Generation of plate tectonics from mantle convection, Am. Geophys. Union Chapman Conf. on History and Dynamics of Global Plate Motions, Marshall, CA, 1997.
[16] B.H. Hager, R.J. O'Connell, A simple global model of plate dynamics and mantle convection, J. Geophys. Res. 86 (1981) 4843–4867.
[17] S. Balachandar, D.A. Yuen, D.M. Reuteler, Localization of toroidal motion and shear heating in 3-D high Rayleigh number convection with temperature-dependent viscosity, Geophys. Res. Lett. 22 (1995) 477–480.
[18] G. Schubert, D.L. Turcotte, One-dimensional model of shallow mantle convection, J. Geophys. Res. 77 (1972) 945–951.
[19] S.-I. Karato, Grain growth kinetics in olivine aggregates, Tectonophysics 168 (1989) 255–273.
[20] K.P. Furlong, Thermal–rheological evolution of the upper mantle and the development of the San Andreas Fault system, Tectonophysics 223 (1993) 149–164.
[21] M. Kameyama, D.A. Yuen, H. Fujimoto, The interaction of viscous heating with grain-size dependent rheology in the formation of localized slip zones, Geophys. Res. Lett. (1997, in press).
[22] A. Lenardic, W.M. Kaula, Self-lubricated mantle convection: Two-dimensional models, Geophys. Res. Lett. 21 (1994) 1707–1710.
[23] J.B. Brady, Diffusion data for silicate minerals, glasses, and liquids, in: Mineral Physics and Crystallography: A Handbook of Physical Constants, AGU Reference Shelf 2, Am. Geophys. Union, Washington, DC, 1995, pp. 269–290.
[24] J.A. Whitehead, R.F. Gans, A new, theoretically tractable earthquake model, Geophys. J.R. Astron. Soc. 39 (1974) 11–28.
[25] S. Zhang, D.A. Yuen, Intense local toroidal motion generated

by variable viscosity compressible convection in 3-D spherical shell, Geophys. Res. Lett. 23 (1996) 3135–3138.
[26] B. Dodd, Y. Baiy, Ductile Fracture and Ductility, Academic Press, New York, NY, 1987, 309 pp.
[27] P.F. Thomason, Ductile Fracture of Metals, Pergamon, Oxford, 1989, 219 pp.
[28] K. Regenauer-Lieb, Dilatant plasticity applied to Alpine collision: Ductile void growth in the intraplate area beneath the Eifel volcanic field, J. Geodyn. (1997, in press).
[29] G.K. Batchelor, An Introduction to Fluid Dynamics, Cambridge University Press, Cambridge, 1967.
[30] M. Spiegelman, pers. commun., 1997
[31] M. Spiegelman, Physics of melt extraction: Theory, implications and applications, Philos. Trans. R. Soc. London, Ser. A 342 (1993) 23–41.
[32] Z. Reches, D.A. Lockner, Nucleation and growth of faults in brittle rocks, J. Geophys. Res. 99 (1994) 18159–18173.
[33] A. Needleman, V. Tvergaard, Analyses of plastic flow deformation in metals, Appl. Mech. Rev. 45 (1992) 3–18.
[34] K.K. Mathur, A. Needleman, V. Tvergaard, Three dimensional analysis of dynamic ductile crack growth in a thin plate, J. Mech. Phys. Solids 44 (1996) 439–464.
[35] N.H. Sleep, Application of a unified rate and state friction theory to the mechanics of fault zones with strain localization, J. Geophys. Res. 102 (1997) 2875–2895.
[36] D. Bercovici, P. Wessel, A continuous kinematic model of plate tectonic motions, Geophys. J. Int. 119 (1994) 595–610.
[37] D.C. Tozer, Heat transfer and planetary evolution, Geophys. Surv. 7 (1985) 213–246.
[38] W.M. Kaula, Venus: A contrast in evolution to Earth, Science 247 (1990) 1191–1196.
[39] W.A. Duffield, A naturally occurring model of global plate tectonics, J. Geophys. Res. 77 (1972) 2543–2555.
[40] D.W. Oldenburg, J.N. Bruhne, Ridge transform fault spreading pattern in freezing wax, Science 178 (1972) 301–304.